

# TNF- $\alpha$ Signals Through PKC $\zeta$ /NF- $\kappa$ B to Alter the Tight Junction Complex and Increase Retinal Endothelial Cell Permeability

Célia A. Avelaira,<sup>1,2</sup> Cheng-Mao Lin,<sup>2</sup> Steven F. Abcouwer,<sup>2,3,4</sup> António F. Ambrósio,<sup>1,5</sup> and David A. Antonetti<sup>2,4</sup>

**OBJECTIVE**—Tumor necrosis factor- $\alpha$  (TNF- $\alpha$ ) and interleukin-1 beta (IL-1 $\beta$ ) are elevated in the vitreous of diabetic patients and in retinas of diabetic rats associated with increased retinal vascular permeability. However, the molecular mechanisms underlying retinal vascular permeability induced by these cytokines are poorly understood. In this study, the effects of IL-1 $\beta$  and TNF- $\alpha$  on retinal endothelial cell permeability were compared and the molecular mechanisms by which TNF- $\alpha$  increases cell permeability were elucidated.

**RESEARCH DESIGN AND METHODS**—Cytokine-induced retinal vascular permeability was measured in bovine retinal endothelial cells (BRECs) and rat retinas. Western blotting, quantitative real-time PCR, and immunocytochemistry were performed to determine tight junction protein expression and localization.

**RESULTS**—IL-1 $\beta$  and TNF- $\alpha$  increased BREC permeability, and TNF- $\alpha$  was more potent. TNF- $\alpha$  decreased the protein and mRNA content of the tight junction proteins ZO-1 and claudin-5 and altered the cellular localization of these tight junction proteins. Dexamethasone prevented TNF- $\alpha$ -induced cell permeability through glucocorticoid receptor transactivation and nuclear factor-kappaB (NF- $\kappa$ B) transrepression. Preventing NF- $\kappa$ B activation with an inhibitor  $\kappa$ B kinase (IKK) chemical inhibitor or adenoviral overexpression of inhibitor  $\kappa$ B alpha (I $\kappa$ B $\alpha$ ) reduced TNF- $\alpha$ -stimulated permeability. Finally, inhibiting protein kinase C zeta (PKC $\zeta$ ) using both a peptide and a novel chemical inhibitor reduced NF- $\kappa$ B activation and completely prevented the alterations in the tight junction complex and cell permeability induced by TNF- $\alpha$  in cell culture and rat retinas.

**CONCLUSIONS**—These results suggest that PKC $\zeta$  may provide a specific therapeutic target for the prevention of vascular permeability in retinal diseases characterized by elevated TNF- $\alpha$ , including diabetic retinopathy. *Diabetes* 59:2872–2882, 2010

From the <sup>1</sup>Centre of Ophthalmology and Vision Sciences, Institute of Biomedical Research in Light and Image (IBILI), Faculty of Medicine, University of Coimbra, Coimbra, Portugal; the <sup>2</sup>Department of Cellular and Molecular Physiology, Penn State Hershey College of Medicine, Hershey, Pennsylvania; the <sup>3</sup>Department of Surgery, Penn State Milton S. Hershey Medical Center, Hershey, Pennsylvania; the <sup>4</sup>Department of Ophthalmology, Penn State Hershey Eye Center, Hershey, Pennsylvania; and the <sup>5</sup>Centre for Neuroscience and Cell Biology, Department of Zoology, University of Coimbra, Coimbra, Portugal.

Corresponding author: Célia A. Avelaira, caveleira@ibili.uc.pt.

Received 30 October 2009 and accepted 28 July 2010. Published ahead of print at <http://diabetes.diabetesjournals.org> on 6 August 2010. DOI: 10.2337/db09-1606.

© 2010 by the American Diabetes Association. Readers may use this article as long as the work is properly cited, the use is educational and not for profit, and the work is not altered. See <http://creativecommons.org/licenses/by-nc-nd/3.0/> for details.

The costs of publication of this article were defrayed in part by the payment of page charges. This article must therefore be hereby marked "advertisement" in accordance with 18 U.S.C. Section 1734 solely to indicate this fact.

The cause of vision loss in diabetic retinopathy is complex and remains incompletely understood; however, changes in blood vessel permeability and macular edema are associated with loss of visual acuity (1–5), with center point thickness and fluorescein leakage combined with age accounting for 33% of the variation in visual acuity (5). A growing body of evidence suggests that diabetic retinopathy includes a neuroinflammatory component, with increased expression of cytokines, microglia activation, leukostasis, and vascular permeability (6–9). Increased levels of interleukin-1 beta (IL-1 $\beta$ ) and tumor necrosis factor- $\alpha$  (TNF- $\alpha$ ) have been detected in the vitreous of diabetic patients with proliferative diabetic retinopathy (10,11) and in diabetic rat retinas (6,7,12). Moreover, intravitreal administration of IL-1 $\beta$  increases vascular permeability, associated with nuclear factor-kappaB (NF- $\kappa$ B) activation, increased leukocyte adhesion, and retinal capillary cell death (13,14). TNF- $\alpha$  also increases leukocyte adhesion to retinal endothelium (15) and blood–retinal barrier (BRB) permeability (16). The inhibition of TNF- $\alpha$  with etanercept, a soluble TNF- $\alpha$  receptor, inhibits NF- $\kappa$ B activation, leukostasis, and BRB breakdown in diabetic rat retinas (12). Altogether, these findings indicate that proinflammatory cytokines contribute to vascular permeability in diabetic retinopathy.

Changes in retinal vascular permeability may result from alterations of the tight junction complex. Tight junctions are composed of a combination of more than 40 proteins including the transmembrane proteins occludin, the claudin family, and the junction adhesion molecule (JAM) family, several peripheral membrane-associated proteins, including members of the *zonula occludens* (ZO) family, and several regulatory proteins (17). To date, evidence has been provided for the presence of occludin, claudin-5, ZO-1, and JAM-A in retinal vascular endothelium (18–21). Changes in occludin content, localization, and phosphorylation occur in response to vascular endothelial growth factor (VEGF) regulating endothelial permeability (18,19,22–24). Gene deletion studies have shown claudin-5 to be essential for blood–brain barrier function (25), and likely for the BRB as well. Recent studies demonstrated that ZO proteins are essential for the formation and organization of tight junction complex assembly (26,27). Therefore, changes in occludin, claudin-5, or ZO-1 likely contribute to alterations in endothelial permeability, in response to inflammatory cytokines.

Although several studies support the involvement of proinflammatory cytokines in BRB breakdown in diabetes, little attention has been given to the molecular mecha-

nisms involved. Therefore, this study was designed to test the hypothesis that alterations to the tight junction protein complex confer endothelial permeability in response to TNF- $\alpha$  and to determine the signaling pathways underlying TNF- $\alpha$ -induced permeability.

TNF- $\alpha$  was shown to regulate permeability in an NF- $\kappa$ B-dependent mechanism by downregulating both claudin-5 and ZO-1 expression. Further, protein kinase C zeta (PKC $\zeta$ ) activity is essential for TNF- $\alpha$ -induced endothelial permeability, partly through NF- $\kappa$ B activation, suggesting that targeting PKC $\zeta$  may provide a novel therapy to control retinal vascular permeability.

## RESEARCH DESIGN AND METHODS

Materials used to carry out the experiments are described in the supplementary Materials and Methods in the online appendix available at <http://diabetes.diabetesjournals.org/cgi/content/full/db09-1606/DC1>.

**Primary bovine retinal endothelial cell culture.** Bovine retinal endothelial cells (BRECs) were isolated and grown as previously described (28), except medium was supplemented with 8  $\mu$ g/ml tylosin. For experimentation, BRECs were grown to confluence and then cell culture media was changed to MCDB-131 medium supplemented with 1% FBS, 0.01 ml/ml antibiotic/antimycotic, and 8  $\mu$ g/ml tylosin for one day and exposed to IL-1 $\beta$  or TNF- $\alpha$ .

**Measurement of BREC permeability.** BREC monolayer permeability to 70 kDa rhodamine isothiocyanate dextran (Sigma-Aldrich, St. Louis, MO) was measured exactly as described previously (24). The average  $P_o$  for control conditions was  $2.77 \times 10^{-6}$  cm/s.

**Animal model.** Male Sprague-Dawley rats (Charles River Laboratories, Wilmington, MA) weighing 150–175 g were used to evaluate retinal vascular permeability and tight junction proteins localization in retinal blood vessels. Animals were housed under a 12-h light/dark cycle with free access to water and a standard rat chow. All experiments were conducted in accordance with the Association for Research in Vision and Ophthalmology (ARVO) Statement for the Use of Animals in Ophthalmic and Vision Research, and were approved and monitored by the Institutional Animal Care and Use Committee (IACUC) at the Penn State College of Medicine. Under anesthesia (66.7 mg/kg ketamine and 6.7 mg/kg xylazine), the animal received an intravitreal injection of TNF- $\alpha$  or vehicle (2.5  $\mu$ l/eye) with a 5  $\mu$ l Hamilton syringe (Hamilton Company, Reno, NV) through a puncture created by a 32-gauge needle. The animals were assessed for retinal permeability with Evans blue assay, 24 h after receiving the intravitreal injection of either PBS with 1% BSA, 10 ng TNF- $\alpha$ , 280 ng PKC $\zeta$ I-1, or TNF- $\alpha$  plus PKC $\zeta$ I-1. In a separate study, retinas were harvested 4 h after injection, immunolabeled for tight junction proteins, and analyzed by confocal microscopy.

**Evans blue assay.** Accumulation of the albumin binding dye Evans blue was used to assess changes in retinal vascular permeability. Evans blue dye accumulation in the retina was quantified using a published protocol (29), with normalization to blood plasma after 2-h circulation and expressed as microliters of plasma per gram of retina (dry weight) per hour of circulation.

**Assessment of cell viability.** The LIVE viability assay (Molecular Probes, Invitrogen, Carlsbad, CA) was used for the assessment of cell viability according to manufacturer's instructions, as described in the supplementary Materials and Methods.

**Caspase-3/7 activity assay.** Caspase-3/7 activity was measured by the Apo-ONE Homogenous caspase-3/7 assay (Promega, Madison, WI), according to the manufacturer's instructions, as briefly described in the supplementary Materials and Methods.

**Western blotting.** Western blotting of cellular lysates was performed as described in the supplementary Materials and Methods.

**RNA extraction and reverse transcription.** RNA extraction and reverse transcription were performed as described in the supplementary Materials and Methods.

**Quantitative real-time PCR.** Quantitative real-time PCR (qPCR) analysis was performed using the 7,900 HT Sequence Detection System in 384-well optical plates using TaqMan Universal PCR Master Mix Assay-on-Demand and Assay-by-Design primers and probes (Applied Biosystems) as previously described (30). Primer/probes used were as follows: claudin-5 Bt03288088\_s1, occludin Bt03255225\_m1, IL-8 Bt03211907\_g1, and bovine ZO-1 specific primers 5'-AGAAAGATGTTTATCGTCGCATCGT-3' (forward), 5'-ATTCCCTCTCATATCAAAATGGGTTCTGA-3' (reverse), and 6-carboxy-fluorescein (FAM) 5'-ACCCACATCGGATTCT-3' minor groove binding (MGB) probe. For each sample, qPCR were performed in triplicate and relative quantities were calculated using ABI SDS 2.0 RQ software and the  $2^{-\Delta\Delta Ct}$  analysis method

(31), with glyceraldehyde-3-phosphate dehydrogenase (Bt03210919\_g1) as the endogenous control.

**Immunocytochemistry.** Tight junction protein cellular localization was evaluated by immunocytochemistry, as previously described (32). Cells were incubated with a rat anti-ZO-1 monoclonal antibody culture supernatant (1:5), rabbit polyclonal anti-claudin-5 (1:500), or anti-occludin (1:300) antibodies overnight at 4°C. Primary antibodies were detected with Alexa Fluor 647-conjugated anti-rat IgG (Molecular Probes, Invitrogen) or Cy3-conjugated anti-rabbit IgG secondary antibodies (Jackson ImmunoResearch Laboratories, West Grove, PA). Coverslips were mounted onto slides using Aqua Poly/Mount (Aquamount; Polysciences, Warrington, PA) and analyzed in a Leica TCS SP2 AOBs confocal microscope. Ten confocal Z-stacks were collected over a depth of 2.56  $\mu$ m and projected onto one image. ZO-1 and occludin localization in retinal vessels were assessed by immunohistochemistry in whole retinas, as described previously (33). The retinas were incubated with monoclonal anti-occludin (1:50) and polyclonal anti-ZO-1 (1:50) antibodies for three days at 4°C. Primary antibodies were detected with Cy2-conjugated anti-mouse IgG and Cy3-conjugated anti-rabbit IgG secondary antibodies (Jackson ImmunoResearch Laboratories) for 24 h at 4°C. After incubation, retinas were washed, mounted in slides with Aqua Poly/Mount, and analyzed on a Leica TCS SP2 AOBs confocal microscope.

**Adenovirus-mediated I $\kappa$ B $\alpha$  overexpression.** I $\kappa$ B $\alpha$  was expressed using the AdEasy adenoviral vector system, as described (34). Subconfluent cells were transduced with adenovirus expressing I $\kappa$ B $\alpha$  (AdI $\kappa$ B $\alpha$ ) or with an empty expression cassette as control (AdEmpty) at a multiplicity of infection of 20,000 for 6 h in MCDB complete medium. After incubation, cells were washed and MCDB media supplemented with 1% serum was added for a further 24 h. Successful viral infection was followed by fluorescence microscopy because the AdEasy vector contains a green fluorescent protein (GFP) cassette incorporated into the viral vector. More than 80% of the cells expressed detectable amounts of GFP after 30 h of adenoviral infection.

**Luciferase reporter assay.** A 293T/NF $\kappa$ B-luc stable reporter cell line (Panomics-Affymetrix, Fremont, CA) was used to evaluate NF- $\kappa$ B transcription factor activity. These cells maintain a chromosomal integrated luciferase reporter gene regulated by multiple copies of the NF- $\kappa$ B response element. After treatments, cells were harvested and lysed with Passive Lysis Buffer (Promega), and the luciferase activity was measured using the Dual-Luciferase Reporter Assay system (Promega) according to manufacturer's instructions. Luciferase activity was normalized to the total protein content of each sample.

**Statistical analysis.** Results are expressed as mean  $\pm$  SEM. Data were analyzed using Student *t* test or one-way ANOVA followed by Dunnett or Bonferroni post hoc test. A value of  $P < 0.05$  was considered significant. Prism 4.0 (GraphPad Software, San Diego, CA) was used for all statistical analysis.

## RESULTS

**IL-1 $\beta$  and TNF- $\alpha$  increase BREC permeability.** BRECs grown on transwell filters were exposed to increasing concentrations and various times of IL-1 $\beta$  and TNF- $\alpha$ , and the monolayer permeability was evaluated. IL-1 $\beta$  significantly increased cell permeability at a concentration of 10 ng/ml ( $220.3 \pm 34.2\%$  of control; Fig. 1A), and this effect was statistically significant after 24 h of treatment (Fig. 1B). Similarly, TNF- $\alpha$  increased cell permeability in a concentration- and time-dependent manner. However, TNF- $\alpha$  was maximally effective at a concentration of 5 ng/ml ( $365.3 \pm 47.8\%$  of control, Fig. 1C) and at a shorter time point than IL-1 $\beta$  (6 h, Fig. 1D). To ensure that the increase in permeability induced by the cytokines was not due to cell death, the effect of IL-1 $\beta$  and TNF- $\alpha$  on BREC viability was evaluated using IL-1 $\beta$  at 10 ng/ml and TNF- $\alpha$  at 5 ng/ml. IL-1 $\beta$  had no effect on cell viability. TNF- $\alpha$ -induced a significant decrease in cell viability after 24 h of treatment ( $70.9 \pm 2.6\%$  of control), but no effect was observed after 6 h of exposure (Fig. 1E). The effect of IL-1 $\beta$  and TNF- $\alpha$  on caspase-3/7 activity, a marker of apoptosis, was also evaluated. IL-1 $\beta$  had no effect on caspase-3/7 activity, whereas TNF- $\alpha$  induced a significant increase in caspase-3/7 activity, but again only after 24 h of exposure (Fig. 1F). Therefore, the increase in cell permeability induced by TNF- $\alpha$  after 6 h of exposure was not due to cell death. Because the effect of TNF- $\alpha$  was more robust than that of IL-1 $\beta$ , the molecular mechanisms under-

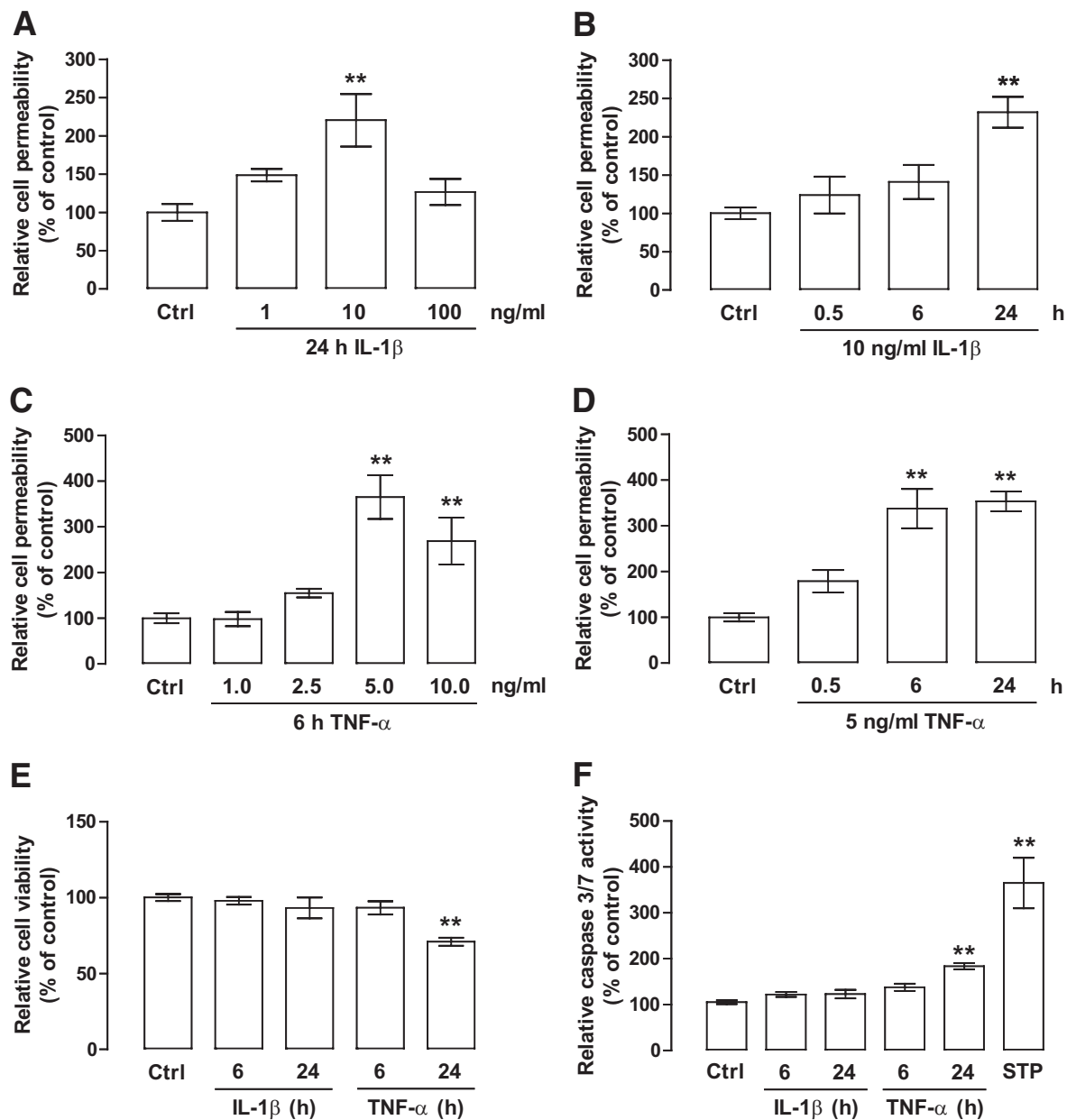


**FIG. 1.** IL-1 $\beta$  and TNF- $\alpha$  increase retinal endothelial cell permeability. *A–D:* BRECs were grown to confluence on transwell filters and then exposed to IL-1 $\beta$  or TNF- $\alpha$  in a concentration- and time-dependent manner. The monolayer permeability to 70 kDa dextran was measured as described in RESEARCH DESIGN AND METHODS. *A:* Cells were treated with 1, 10, and 100 ng/ml IL-1 $\beta$  for 24 h. *B:* Cells were treated with 10 ng/ml IL-1 $\beta$  for 0.5, 6, and 24 h. *C:* Cells were treated with 1, 2.5, 5, and 10 ng/ml TNF- $\alpha$  for 6 h. *D:* Cells were treated with 5 ng/ml TNF- $\alpha$  for 0.5, 6, and 24 h. *E* and *F:* IL-1 $\beta$  and TNF- $\alpha$  effect on cell viability. BRECs were treated with 10 ng/ml IL-1 $\beta$  or 5 ng/ml TNF- $\alpha$  for 6 and 24 h. *E:* Relative cell viability was measured by calcein AM cleavage by live cells. *F:* Retinal endothelial cell apoptosis was evaluated by caspase-3/7 activation. As a positive control of apoptosis induction, cells were treated with 100 nmol/l staurosporine (STP) for 6 h. The results represent the mean  $\pm$  SEM of at least four independent experiments and are expressed relative to control (Ctrl). \*\* $P < 0.01$ , significantly different from control as determined by ANOVA followed by Dunnett post hoc test.

lying TNF- $\alpha$ -induced retinal endothelial cell permeability were further investigated.

**TNF- $\alpha$  alters tight junction protein content and localization.** To determine the effect of TNF- $\alpha$  on expression of specific tight junction proteins, BRECs were exposed to 5 ng/ml TNF- $\alpha$  for 0.5 and 6 h and the protein contents of ZO-1, claudin-5, and occludin were determined by Western blotting. TNF- $\alpha$  significantly decreased ZO-1 content ( $58.2 \pm 6.5\%$  of control) after 6 h of exposure (Fig. 2A). Claudin-5 content was rapidly reduced after 0.5 h of treatment ( $70.8 \pm 7.0\%$  of control, Fig. 2B), and 6 h of TNF- $\alpha$  exposure further downregulated claudin-5 content

( $57.6 \pm 8.7\%$  of control). In contrast, TNF- $\alpha$  increased occludin content ( $130.6 \pm 6.6\%$  of control; Fig. 2C). To determine whether alterations in protein content were due to changes in mRNA expression, total mRNA content was evaluated by qPCR 6 h after TNF- $\alpha$  exposure. TNF- $\alpha$  significantly decreased ZO-1 ( $74.6 \pm 3.3\%$  of control; Fig. 2D) and claudin-5 mRNA content ( $80.9 \pm 5.7\%$  of control; Fig. 2E) but induced a twofold increase in occludin mRNA (Fig. 2F). To investigate whether TNF- $\alpha$  alters the tight junction complex at the cell membrane, the cellular localization of the tight junction proteins were evaluated by immunocytochemistry and confocal microscopy. In con-

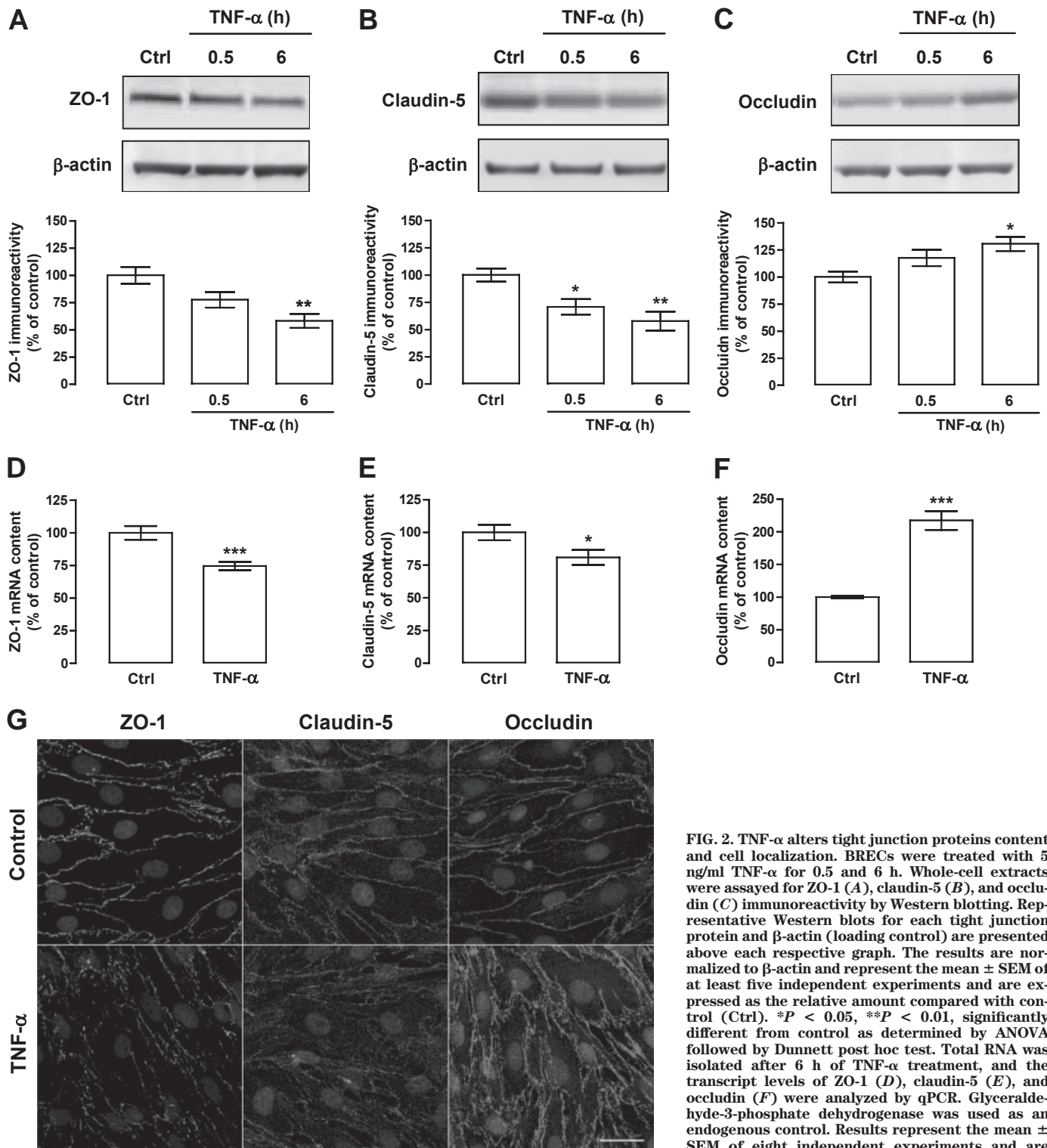


**FIG. 2.** TNF- $\alpha$  alters tight junction proteins content and cell localization. BRECs were treated with 5 ng/ml TNF- $\alpha$  for 0.5 and 6 h. Whole-cell extracts were assayed for ZO-1 (A), claudin-5 (B), and occludin (C) immunoreactivity by Western blotting. Representative Western blots for each tight junction protein and  $\beta$ -actin (loading control) are presented above each respective graph. The results are normalized to  $\beta$ -actin and represent the mean  $\pm$  SEM of at least five independent experiments and are expressed as the relative amount compared with control (Ctrl). \* $P$  < 0.05, \*\* $P$  < 0.01, significantly different from control as determined by ANOVA followed by Dunnett post hoc test. Total RNA was isolated after 6 h of TNF- $\alpha$  treatment, and the transcript levels of ZO-1 (D), claudin-5 (E), and occludin (F) were analyzed by qPCR. Glyceraldehyde-3-phosphate dehydrogenase was used as an endogenous control. Results represent the mean  $\pm$  SEM of eight independent experiments and are expressed as the relative amount compared with control conditions. \* $P$  < 0.05, \*\*\* $P$  < 0.001, significantly different from control as determined by Student  $t$  test. G: Cells were immunolabeled for ZO-1, claudin-5, and occludin 6 h after TNF- $\alpha$  treatment, and 10 confocal Z-stacks were taken through 2.56  $\mu$ m and projected into one image. Arrows indicate continuous staining at cell borders. These results are representative of four independent experiments. Scale bar, 25  $\mu$ m.

control conditions, ZO-1, claudin-5, and occludin immunoreactivity appeared as a near continuous staining at the cell border (Fig. 2G and supplementary Fig. 1, available in an online appendix). Upon TNF- $\alpha$  treatment, a loss of both ZO-1 and claudin-5 immunostaining was observed, leading to a fragmented border staining, although the

effect on ZO-1 was more pronounced. Also, a diffuse cytoplasmic distribution of claudin-5 and occludin was observed in TNF- $\alpha$ -treated cells. After TNF- $\alpha$  treatment, occludin staining increased, and it was irregularly distributed at the cell border (Fig. 2G and supplementary Fig. 1).

effect on ZO-1 was more pronounced. Also, a diffuse cytoplasmic distribution of claudin-5 and occludin was observed in TNF- $\alpha$ -treated cells. After TNF- $\alpha$  treatment, occludin staining increased, and it was irregularly distributed at the cell border (Fig. 2G and supplementary Fig. 1).

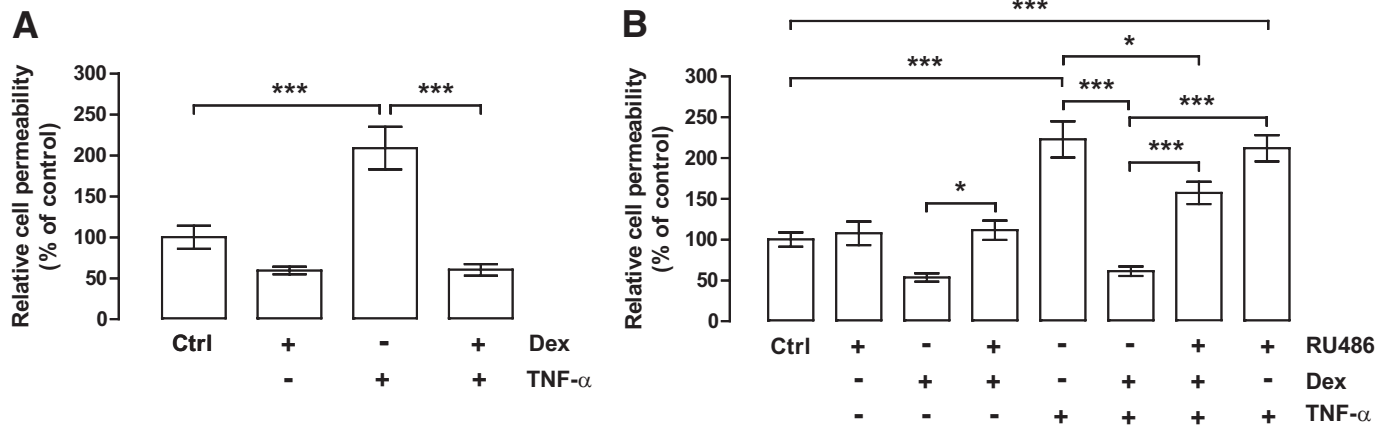


**FIG. 3.** Dexamethasone prevents TNF-α-induced cell permeability through transactivation of the glucocorticoid receptor. **A:** BRECs were grown to confluence on transwell filters and treated with 50 ng/ml dexamethasone (Dex) 18 h before TNF-α treatment (5 ng/ml, 6 h). **B:** Cells were treated with 5 μmol/l RU486 1 h before Dex treatment. The monolayer permeability to 70 kDa dextran was measured as described in RESEARCH DESIGN AND METHODS. The results represent the mean ± SEM of at least seven independent experiments and are expressed relative to control (Ctrl). \**P* < 0.05, \*\*\**P* < 0.001, significantly different as determined by ANOVA followed by Bonferroni post hoc test.

**Dexamethasone prevents TNF-α-induced BREC permeability.** The effect of the glucocorticoid dexamethasone on TNF-α-induced endothelial permeability was determined. BRECs were treated with 50 ng/ml dexamethasone 18 h before TNF-α treatment. The increase in cell permeability induced by TNF-α was completely prevented by dexamethasone (Fig. 3A). To investigate if the effect of dexamethasone was dependent on transcriptional activation by the glucocorticoid receptor, BRECs were pretreated with 5 μmol/l RU486, a glucocorticoid receptor antagonist that inhibits the transactivation function of this receptor (35). A 1-h pretreatment of RU486 before the addition of dexamethasone significantly reduced the protective effect of dexamethasone on TNF-α-induced cell permeability (Fig. 3B). RU486 alone had no effect on permeability and did not alter the TNF-α response but did prevent the dexamethasone reduction in permeability as previously reported (36). These data show that dexamethasone's protective effect is partially due to glucocorticoid receptor transactivation but also suggest that transrepression of TNF-α-responsive transcription factors also contributes to the inhibition of TNF-α-induced cell permeability.

**Dexamethasone prevents TNF-α-induced alterations in tight junction proteins.** The effect of dexamethasone on TNF-α-induced changes in tight junction protein content and cellular localization was also evaluated. Dexamethasone alone significantly increased ZO-1, claudin-5, and occludin protein content (Fig. 4). TNF-α decreased ZO-1 and claudin-5 protein content and these effects were prevented by dexamethasone pretreatment (Fig. 4A and B), whereas dexamethasone and TNF-α treatment yielded an additive threefold increase in occludin protein content (Fig. 4C). Dexamethasone increased ZO-1, claudin-5, and occludin staining at the cell border and prevented the TNF-α-induced fragmentation of these tight junction proteins (Fig. 4D and supplementary Fig. 1).

**NF-κB inhibition reduces TNF-α-induced cell permeability.** The involvement of NF-κB activation in TNF-α-induced endothelial permeability was investigated. BRECs were exposed to 1 μmol/l IKK VII, an IκB kinase complex inhibitor, 30 min before TNF-α addition. As a control for inhibitor IKK VII effectiveness, TNF-α-induced IκBα phosphorylation by IKK was evaluated. Figure 5A shows that

IκBα phosphorylation was blocked by IKK VII. The TNF-α-induced increase in permeability (275.0 ± 46.7% of control) was significantly reduced by IKK VII (160.5 ± 21.7% of control; Fig. 5B). The effect of adenovirus-mediated overexpression of IκBα on cell permeability was also evaluated. Western blotting was used to confirm the adenovirus-mediated expression of GFP and IκBα 30 h after adenoviral infection. GFP expression was similar in both AdEmpty- and AdIκBα-transduced cells, while IκBα was heavily expressed in AdIκBα-transduced cells compared with AdEmpty-transduced cells (Fig. 5C). The ability of IκBα overexpression to inhibit NF-κB activation was evaluated by examining the TNF-α-induced expression of IL-8 mRNA, a transcriptional target of NF-κB. In both nontransduced and AdEmpty-transduced cells, IL-8 mRNA levels were significantly increased (by 18- and 16-fold, respectively) after 2 h of TNF-α stimulation (Fig. 5D). This increase in IL-8 expression was significantly reduced (by 41%) in AdIκBα-transduced cells, demonstrating that adenovirus-mediated overexpression of IκBα effectively blocked NF-κB activation after TNF-α treatment. Subsequently, the effect of IκBα overexpression on TNF-α-induced cell permeability was determined. In AdEmpty-transduced cells, TNF-α induced a significant increase in cell permeability (273.6 ± 71.0% of control; Fig. 5E), similar to nontransduced cells (Fig. 5E). IκBα overexpression reduced TNF-α-induced permeability to 157.5 ± 5.7% of control. These data suggest that NF-κB activation is necessary for a substantial part of the TNF-α-induced changes in BREC permeability.

**PKCζI-1 inhibits NF-κB activation induced by TNF-α.** PKCζ has a critical role in the activation of the NF-κB pathway (37). To determine whether PKCζ modulates NF-κB activation in retinal endothelial cells induced by TNF-α, the effect of PKCζI-1, a novel PKCζ inhibitor with little or no inhibitory activity on PKCβ or PKCδ (manuscript in preparation), on TNF-α-induced IL-8 mRNA expression, was evaluated. BRECs were treated with 10 μmol/l PKCζI-1 30 min before treatment of cells with TNF-α for 2 h. TNF-α induced a significant 14-fold increase in IL-8 transcripts, which was significantly reduced to 6-fold by PKCζI-1 (Fig. 6A). The effect of PKCζI-1 on TNF-α-induced NF-κB reporter activity was investigated in a 293/NF-κB/luc stable reporter cell line. Cells were

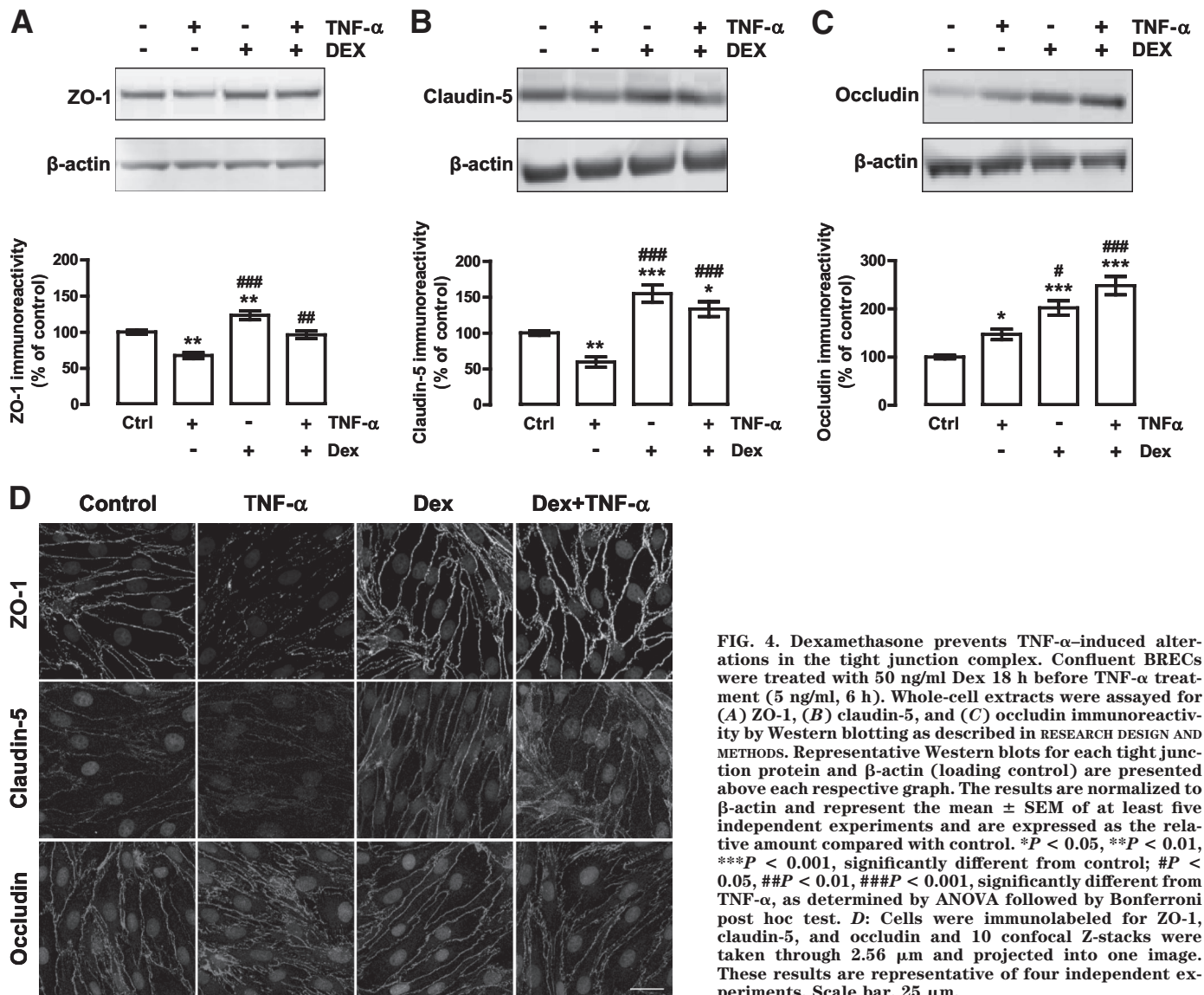


**FIG. 4.** Dexamethasone prevents TNF- $\alpha$ -induced alterations in the tight junction complex. Confluent BRECs were treated with 50 ng/ml Dex 18 h before TNF- $\alpha$  treatment (5 ng/ml, 6 h). Whole-cell extracts were assayed for (A) ZO-1, (B) claudin-5, and (C) occludin immunoreactivity by Western blotting as described in RESEARCH DESIGN AND METHODS. Representative Western blots for each tight junction protein and  $\beta$ -actin (loading control) are presented above each respective graph. The results are normalized to  $\beta$ -actin and represent the mean  $\pm$  SEM of at least five independent experiments and are expressed as the relative amount compared with control. \* $P < 0.05$ , \*\* $P < 0.01$ , \*\*\* $P < 0.001$ , significantly different from control; # $P < 0.05$ , ## $P < 0.01$ , ### $P < 0.001$ , significantly different from TNF- $\alpha$ , as determined by ANOVA followed by Bonferroni post hoc test. **D:** Cells were immunolabeled for ZO-1, claudin-5, and occludin and 10 confocal Z-stacks were taken through 2.56  $\mu$ m and projected into one image. These results are representative of four independent experiments. Scale bar, 25  $\mu$ m.

treated with 10 or 50  $\mu$ M PKC $\zeta$ I-1 30 min before the addition of TNF- $\alpha$  for 6 h, and luciferase activity was determined in whole-cell lysates. The results show that PKC $\zeta$ I-1 significantly decreased TNF- $\alpha$ -induced NF- $\kappa$ B-responsive luciferase expression in these cells (Fig. 6B). These observations suggest that pharmacological inhibition of PKC $\zeta$  reduces NF- $\kappa$ B activation in response to TNF- $\alpha$ .

**TNF- $\alpha$ -induced cell permeability requires PKC $\zeta$ .** PKC $\zeta$  activation can occur downstream of the PI $_3$ K pathway (38), which has been shown to be activated by TNF- $\alpha$  in vascular endothelial cells (39). Therefore, the effect of PI $_3$ K/PKC $\zeta$  pathway inhibition on retinal endothelial cell permeability was investigated. BRECs were treated with 2  $\mu$ M LY294002, a PI $_3$ K inhibitor, 30 min before the treatment with TNF- $\alpha$  for 6 h. The increase in cell permeability induced by TNF- $\alpha$  was significantly inhibited by 56% in the presence of LY294002 (Fig. 7A). Next, BRECs were exposed to 10  $\mu$ M PKC $\zeta$ I-1 or the myristoylated pseudosubstrate inhibitor of PKC $\zeta$  (PKC $\zeta$ p; 250 nmol/l) 30 min prior to TNF- $\alpha$  addition. Both PKC $\zeta$ I-1 and PKC $\zeta$ p completely suppressed the increase in cell permeability induced by TNF- $\alpha$  (Fig. 7B and C). Because conventional

PKC isoforms contribute to the VEGF-induced permeability in retinal endothelial cells (23), the contributions of conventional and novel PKC isoforms for TNF- $\alpha$ -induced cell permeability were also evaluated. BRECs were treated with 5  $\mu$ M BIM I (inhibitor of conventional and novel PKC isoforms) or with 30 nmol/l PKC $\beta$  inhibitor 30 min before TNF- $\alpha$  treatment. These inhibitors had no effect on TNF- $\alpha$ -induced cell permeability (supplementary Fig. 2A and B, available in an online appendix). These results suggest that PKC $\zeta$ , but not conventional and novel PKC isoforms, mediate TNF- $\alpha$ -induced retinal endothelial cell permeability. The effect of PKC $\zeta$  inhibition on tight junction protein content in TNF- $\alpha$ -treated BRECs was also evaluated. The protein content of ZO-1, claudin-5, and occludin was not affected by treatment with PKC $\zeta$ I-1. However, the decrease in ZO-1 and claudin-5 protein levels induced by TNF- $\alpha$  was effectively prevented by PKC $\zeta$ I-1 (Fig. 7E and F). Surprisingly, in the presence of PKC $\zeta$ I-1, TNF- $\alpha$  still caused an increase in occludin protein content, which actually was greater than the effect of TNF- $\alpha$  alone (Fig. 7G).

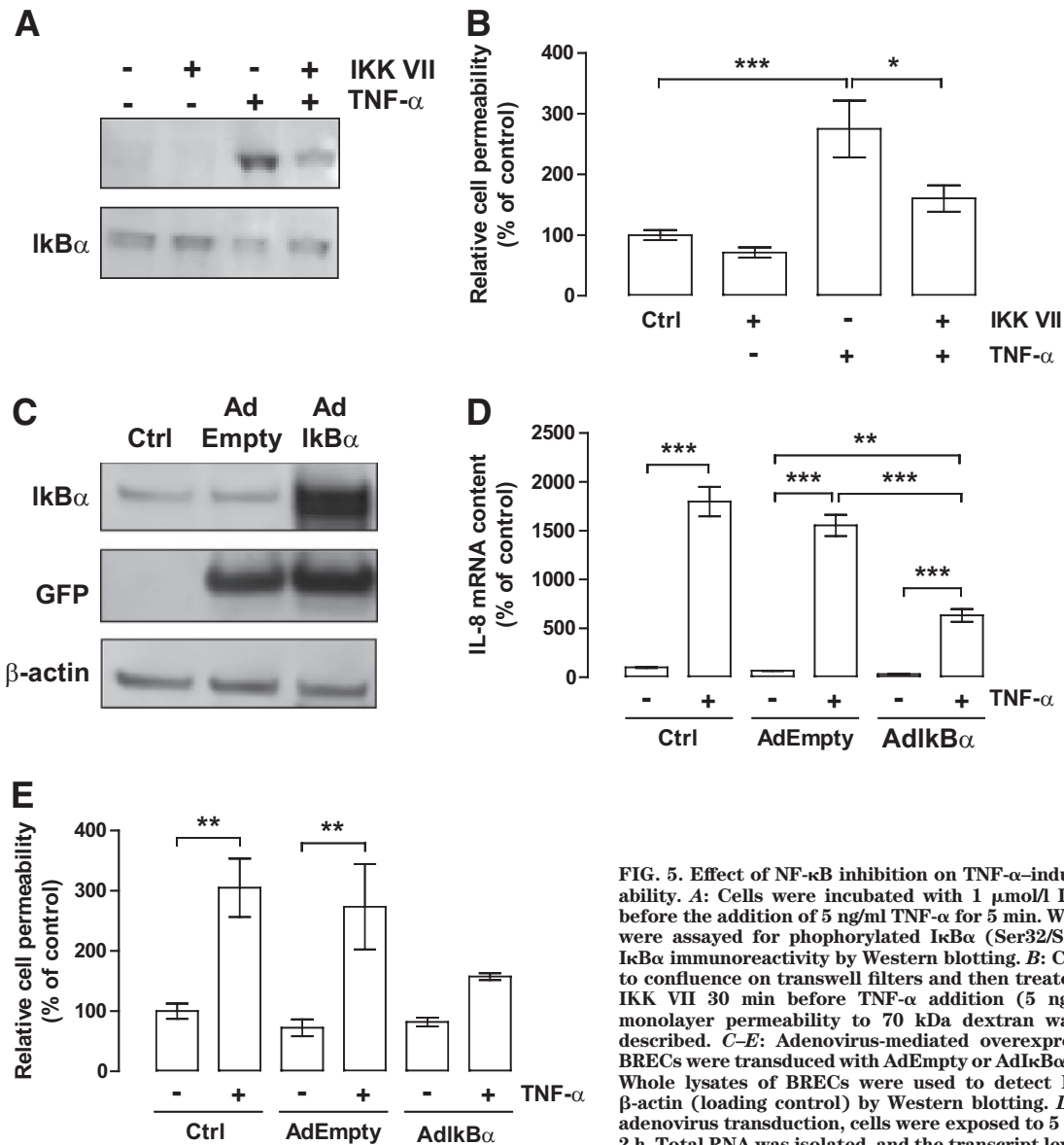


**FIG. 5.** Effect of NF- $\kappa$ B inhibition on TNF- $\alpha$ -induced cell permeability. **A:** Cells were incubated with 1  $\mu$ mol/l IKK VII, 30 min before the addition of 5 ng/ml TNF- $\alpha$  for 5 min. Whole-cell lysates were assayed for phosphorylated I $\kappa$ B $\alpha$  (Ser32/Ser36) and total I $\kappa$ B $\alpha$  immunoreactivity by Western blotting. **B:** Cells were grown to confluence on transwell filters and then treated with 1  $\mu$ mol/l IKK VII 30 min before TNF- $\alpha$  addition (5 ng/ml, 6 h). The monolayer permeability to 70 kDa dextran was measured as described. **C–E:** Adenovirus-mediated overexpression of I $\kappa$ B $\alpha$ . BRECs were transduced with AdEmpty or AdI $\kappa$ B $\alpha$  as described. **C:** Whole lysates of BRECs were used to detect I $\kappa$ B $\alpha$ , GFP, and  $\beta$ -actin (loading control) by Western blotting. **D:** After 28 h of adenovirus transduction, cells were exposed to 5 ng/ml TNF- $\alpha$  for 2 h. Total RNA was isolated, and the transcript levels of IL-8 were analyzed by qPCR. **E:** Cells were grown to confluence on transwell

filters and after 24 h of adenovirus transduction cells were treated with 5 ng/ml TNF- $\alpha$  for 6 h. The monolayer permeability to 70 kDa dextran was measured. The results represent the mean  $\pm$  SEM of at least three independent experiments and are expressed relative to control (Ctrl). \* $P$  < 0.05, \*\* $P$  < 0.01, \*\*\* $P$  < 0.001, significantly different as determined by ANOVA followed by Bonferroni post hoc test.

**PKC $\zeta$ I-1 prevents TNF- $\alpha$ -induced BRB permeability in vivo.** The effect of PKC $\zeta$ I-1 on TNF- $\alpha$ -induced BRB permeability was evaluated in vivo by the Evans blue assay. The injection of TNF- $\alpha$  in the vitreous induced the accumulation of Evans blue (20.30  $\pm$  2.46  $\mu$ l plasma/g/h) as compared with PBS-injected animals (10.25  $\pm$  2.48  $\mu$ l plasma/g/h; Fig. 8A). PKC $\zeta$ I-1 alone had no effect on the accumulation of Evans blue but completely prevented TNF- $\alpha$ -induced accumulation of the dye. To determine the effect of TNF- $\alpha$  injection and PKC $\zeta$  inhibition on retinal vascular tight junction organization, retina whole flat mounts were immunolabeled for ZO-1 and occludin proteins after injection of the cytokine or cytokine with PKC $\zeta$ I-1. In PBS-injected rat eyes, ZO-1 and occludin immunoreactivities were intense and localized at the junctions of the cell membranes of endothelial cells in retinal vessels. In TNF- $\alpha$ -injected eyes, changes in ZO-1 immunostaining were particularly evident, which became markedly reduced and intermittently absent from the cell

borders. These alterations were prevented by cotreatment with PKC $\zeta$ I-1 (Fig. 8B). Consistent with the results obtained with BRECs in culture, the occludin content was not reduced with TNF- $\alpha$  but displayed regions with disorganized cell-border labeling that were reversed by PKC $\zeta$ I-1 treatment.

**DISCUSSION**

Elevated levels of proinflammatory cytokines IL-1 $\beta$  and TNF- $\alpha$  have been detected in the vitreous of diabetic patients with retinopathy (10,11) and in diabetic rat retinas correlated with increased vascular permeability (12,40). However, the mechanisms underlying the effects of IL-1 $\beta$  and TNF- $\alpha$  on retinal microvascular barrier have not been addressed. The results presented herein demonstrate that IL-1 $\beta$  and TNF- $\alpha$  increase retinal endothelial cell permeability and that TNF- $\alpha$  acts through PKC $\zeta$ /NF- $\kappa$ B to reduce the expression and alter the distribution of the tight

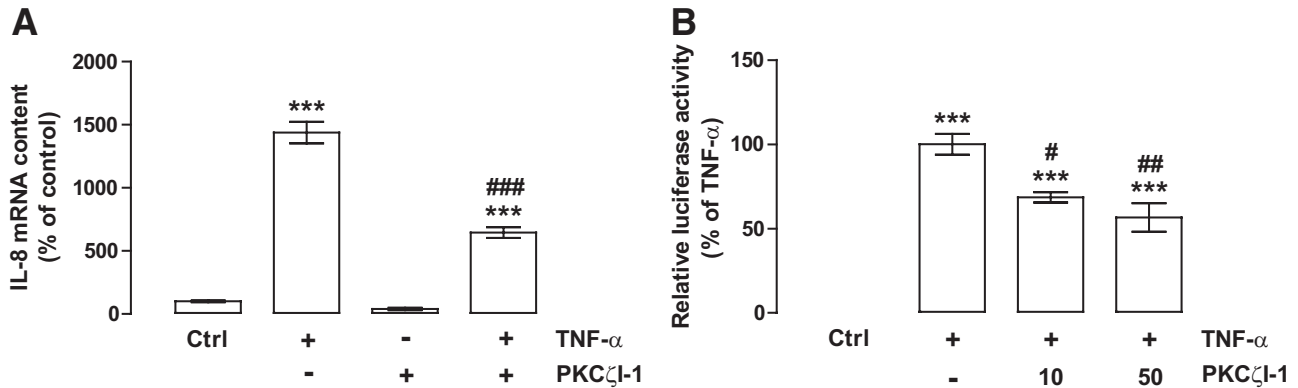


**FIG. 6.** Inhibition of PKC $\zeta$  inhibits NF- $\kappa$ B activation by TNF- $\alpha$ . **A:** BRECs were treated with 10  $\mu$ mol/l PKC $\zeta$ I-1, a PKC $\zeta$  inhibitor, 30 min before the addition of 5 ng/ml TNF- $\alpha$  for 2 h. Total RNA was isolated, and the transcript levels of IL-8 were analyzed by qPCR. The results represent the mean  $\pm$  SEM of six independent experiments and are expressed relative to control (Ctrl). **B:** 293T-NF- $\kappa$ B-luc cells, with a  $\kappa$ B-dependent luciferase reporter gene, were treated with 10 or 50  $\mu$ mol/l PKC $\zeta$ I-1 30 min prior to the addition of TNF- $\alpha$  for 6 h. Cells were harvested, and luciferase activity was determined in whole-cell lysates. The results represent the mean  $\pm$  SEM of four independent experiments and are expressed relative to TNF- $\alpha$ . \*\*\* $P$  < 0.001, significantly different from control; # $P$  < 0.05, ## $P$  < 0.01, ### $P$  < 0.001, significantly different from TNF- $\alpha$ , as determined by ANOVA followed by Bonferroni post hoc test.

junction proteins claudin-5 and ZO-1. Moreover, glucocorticoid treatment completely prevented the TNF- $\alpha$ -induced increase in retinal endothelial cell permeability through both transactivation of the glucocorticoid receptor and transrepression of the NF- $\kappa$ B signaling pathway. Pharmacological inhibition of PKC $\zeta$  reduced NF- $\kappa$ B activation and

prevented TNF- $\alpha$ -induced retinal endothelial cell permeability both in vitro and in vivo.

The increase in retinal vascular permeability is associated with changes in the expression or distribution of the tight junction proteins. The content of occludin and ZO-1 decreases in the retinas of diabetic animals (18,33,41). In

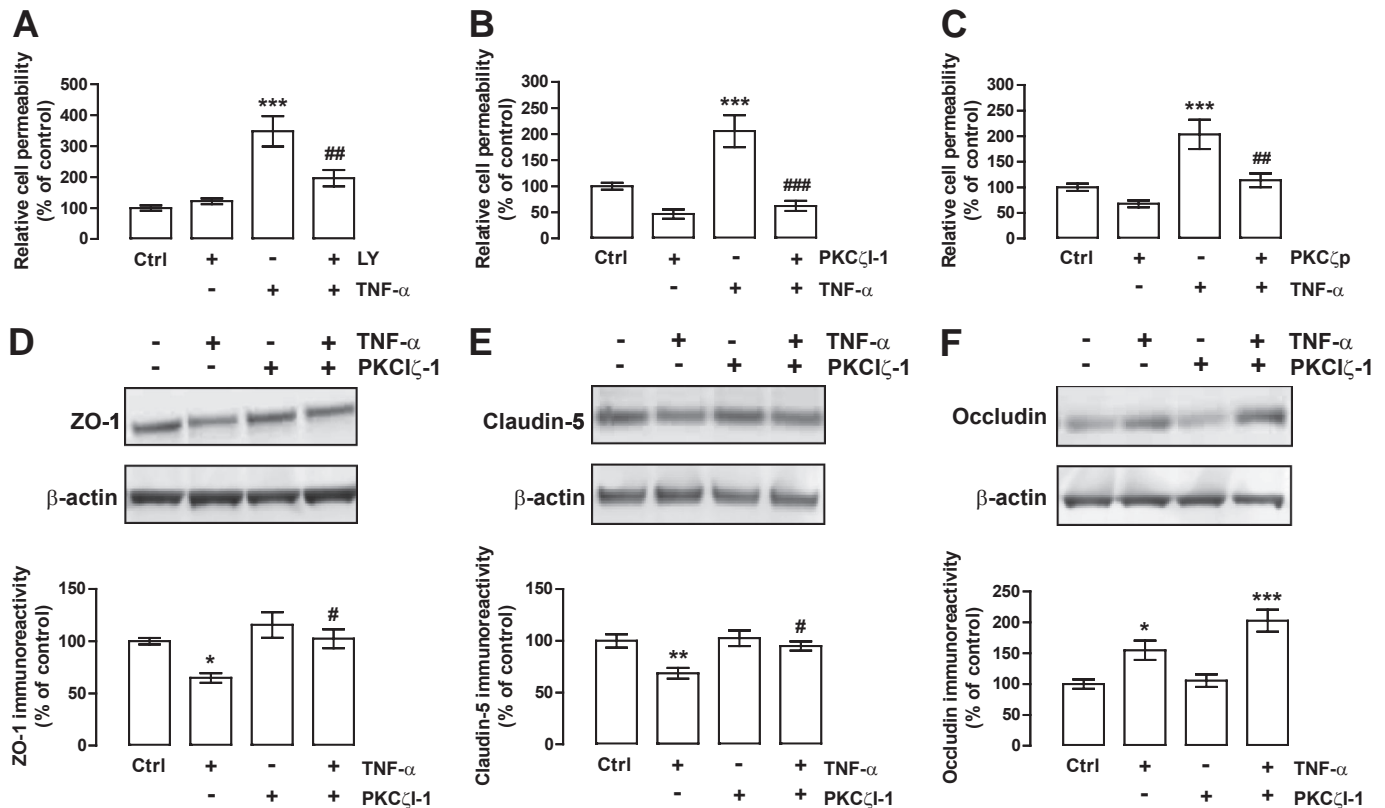


**FIG. 7.** TNF- $\alpha$  increases cell permeability in a PKC $\zeta$ -dependent manner. BRECs were grown to confluence on transwell filters and then treated with (A) 2  $\mu$ mol/l LY294002 (LY), (B) 10  $\mu$ mol/l PKC $\zeta$ I-1, and (C) 250 nmol/l PKC $\zeta$  pseudosubstrate inhibitor (PKC $\zeta$ p). The monolayer permeability to 70 kDa dextran was measured as described. Results represent the mean  $\pm$  SEM of at least five experiments and are expressed relative to Ctrl. **D–F:** PKC $\zeta$ I-1 prevents tight junction complex disruption induced by TNF- $\alpha$ . Whole-cell extracts were assayed for (D) ZO-1, (E) claudin-5, and (F) occludin immunoreactivity by Western blotting. Representative Western blots for each tight junction protein and  $\beta$ -actin (loading control) are presented above each respective graph. The results are normalized to  $\beta$ -actin and represent the mean  $\pm$  SEM of at least eight independent experiments and are expressed as the relative amount compared with control (Ctrl). All inhibitors were added to the cell culture medium 30 min before TNF- $\alpha$  addition (5 ng/ml, 6 h). \* $P$  < 0.05, \*\* $P$  < 0.01, \*\*\* $P$  < 0.001, significantly different from control; # $P$  < 0.05, ## $P$  < 0.01, ### $P$  < 0.001, significantly different from TNF- $\alpha$ , as determined by ANOVA followed by Bonferroni post hoc test.

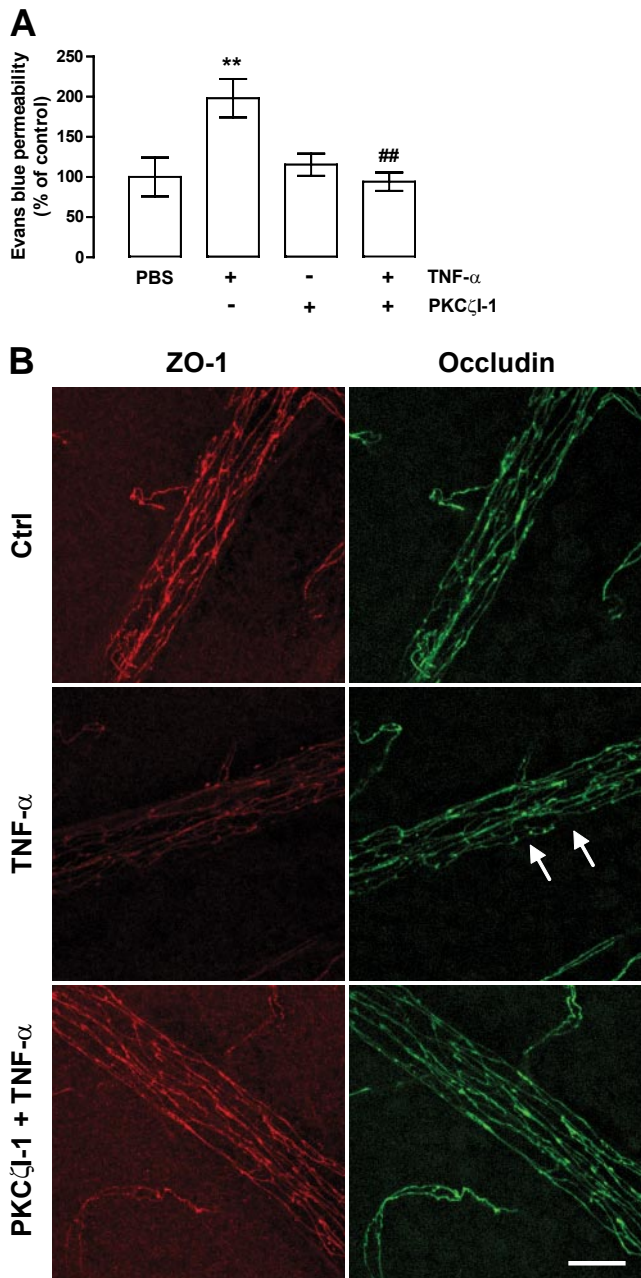


**FIG. 8.** PKC $\zeta$ I-1 prevents TNF- $\alpha$ -induced retinal vascular permeability in vivo. Animals' eyes were injected with PBS with 0.1% BSA, TNF- $\alpha$  (10 ng); PKC $\zeta$ I-1 (280 ng); or with both PKC $\zeta$ I-1 and TNF- $\alpha$ . **A:** Evans blue leakage was evaluated 24 h after intravitreal injections. The results represent the mean  $\pm$  SEM ( $n = 7$ – $8$  animals per group) and are expressed relative to control (Ctrl; PBS-injected eyes). **\*\* $P < 0.01$ ,** significantly different from control; **## $P < 0.01$ ,** significantly different from TNF- $\alpha$ , as determined by ANOVA followed by Bonferroni post hoc test. **B:** PKC $\zeta$ I-1 prevents the alterations in tight junction proteins induced by TNF- $\alpha$  in vivo. Whole retinas were immunolabeled for ZO-1 and occludin 4 h after injection. Images were obtained on a Leica TCS SP2 AOBs confocal microscope and are presented as a maximum projection. Arrows indicate loss and/or discontinuous cell border staining. Scale bar, 25  $\mu$ m. (A high-quality digital representation of this figure is available in the online issue.)

BRECs, TNF- $\alpha$  downregulated ZO-1 and claudin-5 expression and decreased the junctional localization of both proteins, which was associated with an increase in cell permeability. These studies are consistent with previous publications demonstrating reduced claudin-5 gene expression after TNF- $\alpha$  treatment in brain capillary endothe-

lial cells (42,43). However, in these same studies, a decrease in occludin was observed after TNF- $\alpha$  treatment, which contrast the increase in occludin observed in the present study. Further, TNF- $\alpha$  reduced occludin promoter activity in a human intestinal cell line (44). The cause for this difference is unclear but may relate to the use of cell lines versus primary culture or differences in epithelial and endothelial cell types. Regardless, TNF- $\alpha$  consistently reduces both claudin-5 and ZO-1 expression, two tight junction proteins essential for barrier properties.

The effect of TNF- $\alpha$  and VEGF on retinal endothelial permeability is distinct. Occludin becomes phosphorylated on multiple sites after VEGF treatment in a conventional PKC-dependent manner (23) and Ser490 has recently been identified as a phosphorylation site necessary for VEGF-induced permeability (24,45). TNF- $\alpha$  did not lead to an increase in occludin phosphorylation on Ser490 (data not shown) but rather led to an increase in occludin expression. Further, inhibition of conventional or novel PKC isoforms did not prevent TNF- $\alpha$ -induced permeability. These data demonstrate that VEGF and TNF- $\alpha$  alter retinal endothelial barrier properties by distinct molecular mechanisms.

The data presented here suggest that glucocorticoid receptor activation inhibits TNF- $\alpha$ -induced cell permeability through both transactivation and transrepression mechanisms. Inhibition of IKK and adenovirus-mediated overexpression of I $\kappa$ B $\alpha$  blocked the increase in BREC permeability induced by TNF- $\alpha$  treatment. Together, these data demonstrate that TNF- $\alpha$ -induced retinal endothelial cell permeability is mediated, at least in part, by NF- $\kappa$ B. The mechanisms by which NF- $\kappa$ B may regulate cell permeability and the tight junction complex are largely unknown. NF- $\kappa$ B putative binding sites and several E-box sequences were identified within the claudin-5 promoter sequence (43). Recent studies demonstrated that NF- $\kappa$ B induces the expression of Snail and Slug transcription factors (46,47), which repress E-cadherin, occludin, and claudin family members gene expression by binding to specific E-box sequences during epithelial-mesenchymal transition (48–50). These reports suggest the possibility that a similar regulation by transcriptional repressors might also play a role in claudin-5 and ZO-1 expression in retinal endothelial cells.

PKC $\zeta$  has been shown to contribute a critical and selective role in the regulation of NF- $\kappa$ B. In PKC $\zeta$ -deficient mice, NF- $\kappa$ B transcriptional activity as well as the phosphorylation of p65 in response to TNF- $\alpha$  is severely impaired (37). In endothelial cells, the transcriptional activity of NF- $\kappa$ B is dependent on the phosphorylation of the p65 subunit by PKC $\zeta$  (51). The observations that TNF- $\alpha$ -induced increase in IL-8 expression and NF- $\kappa$ B-dependent luciferase reporter expression are inhibited by PKC $\zeta$ I-1 further support the hypothesis that PKC $\zeta$  is important for NF- $\kappa$ B transcriptional activity.

In endothelial cells, PKC $\zeta$  has been shown to be activated by TNF- $\alpha$  (51–53). The mechanism of activation of PKC $\zeta$  remains to be fully clarified, but it has been shown to be an important downstream target of PI $_3$ K (38). TNF- $\alpha$  stimulates PI $_3$ K in endothelial cells through endothelial/epithelial tyrosine kinase induced activation of VEGFR2 (39). Interestingly, this is only a partial activation of VEGFR2 that fails to activate the classical PKC isoforms necessary for VEGF-stimulated permeability (23,54). PI $_3$ K inhibition and inhibition of its downstream target PKC $\zeta$  (38) blocked TNF- $\alpha$ -induced cell permeability, whereas

classical PKC inhibitors failed. Targeting PKC $\zeta$  reduced NF- $\kappa$ B activation and most likely inhibited additional signaling pathways that contribute to the regulation of the tight junction complex and endothelial permeability induced by TNF- $\alpha$ . PKC $\zeta$ I-1 is also effective at blocking VEGF-induced permeability (manuscript in preparation). Then, although VEGF and TNF- $\alpha$  alter the tight junction complex by distinct mechanisms, inhibition of PKC $\zeta$  is a common target for blocking both VEGF- and TNF- $\alpha$ -induced cell permeability. Therefore, targeting PKC $\zeta$  may provide a specific therapeutic option for the prevention of vascular permeability in retinal diseases with elevated TNF- $\alpha$  and VEGF, such as diabetic retinopathy.

#### ACKNOWLEDGMENTS

This study was supported by the Foundation for Science and Technology, Portugal (SFRH/BD/18827/2004), FEDER, National Institutes of Health Grants EY-016413 and EY-012021 (D.A.A.), and the Juvenile Diabetes Research Foundation International (D.A.A.). No potential conflicts of interest relevant to this article were reported.

C.A.A. and A.F.A. researched data, contributed to discussion, wrote the manuscript, and reviewed/edited the manuscript. C.-M.L., S.F.A., and D.A.A. researched data, contributed to discussion, and reviewed/edited the manuscript.

The authors thank Ellen Wolpert and Kristin Gonsar of the Department of Cellular and Molecular Physiology, Penn State College of Medicine, and Rob Brucklacher and Georgina Bixler of the Functional Genomics Core Facility of the Section of Research Resources, Penn State Hershey College of Medicine, for technical assistance.

#### REFERENCES

- Antonetti DA, Barber AJ, Bronson SK, Freeman WM, Gardner TW, Jefferson LS, Kester M, Kimball SR, Krady JK, LaNoue KF, Norbury CC, Quinn PG, Sandirasegarane L, Simpson IA, JDRF Diabetic Retinopathy Center Group. Diabetic retinopathy: seeing beyond glucose-induced microvascular disease. *Diabetes* 2006;55:2401–2411
- Gardner TW, Larsen M, Girach A, Zhi X, on behalf of the Protein Kinase C Diabetic Retinopathy Study (PCK-DRS2) Study Group. Diabetic macular oedema and visual loss: relationship to location, severity and duration. *Acta Ophthalmol* 2009;87:709–713
- Moss SE, Klein R, Klein BE. The 14-year incidence of visual loss in a diabetic population. *Ophthalmology* 1998;105:998–1003
- Sander B, Thornit DN, Colmorn L, Strøm C, Girach A, Hubbard LD, Lund-Andersen H, Larsen M. Progression of diabetic macular edema: correlation with blood retinal barrier permeability, retinal thickness, and retinal vessel diameter. *Invest Ophthalmol Vis Sci* 2007;48:3983–3987
- Diabetic Retinopathy Clinical Research Network, Browning DJ, Glassman AR, Aiello LP, Beck RW, Brown DM, Fong DS, Bressler NM, Danis RP, Kinyoun JL, Nguyen QD, Bhavsar AR, Gottlieb J, Pieramici DJ, Rauser ME, Apte RS, Lim JI, Miskala PH. Relationship between optical coherence tomography-measured central retinal thickness and visual acuity in diabetic macular edema. *Ophthalmology* 2007;114:525–536
- Carmo A, Cunha-Vaz JG, Carvalho AP, Lopes MC. L-arginine transport in retinas from streptozotocin diabetic rats: correlation with the level of IL-1 beta and NO synthase activity. *Vision Res* 1999;39:3817–3823
- Krady JK, Basu A, Allen CM, Xu Y, LaNoue KF, Gardner TW, Levison SW. Minocycline reduces proinflammatory cytokine expression, microglial activation, and caspase-3 activation in a rodent model of diabetic retinopathy. *Diabetes* 2005;54:1559–1565
- Miyamoto K, Khosrof S, Bursell SE, Rohan R, Murata T, Clermont AC, Aiello LP, Ogura Y, Adamis AP. Prevention of leukostasis and vascular leakage in streptozotocin-induced diabetic retinopathy via intercellular adhesion molecule-1 inhibition. *Proc Natl Acad Sci U S A* 1999;96:10836–10841
- Rungger-Brändle E, Dosso AA, Leuenberger PM. Glial reactivity, an early feature of diabetic retinopathy. *Invest Ophthalmol Vis Sci* 2000;41:1971–1980
- Abu el Asrar AM, Maimone D, Morse PH, Gregory S, Reder AT. Cytokines in the vitreous of patients with proliferative diabetic retinopathy. *Am J Ophthalmol* 1992;114:731–736
- Demircan N, Safran BG, Soylu M, Ozcan AA, Sizmaz S. Determination of vitreous interleukin-1 (IL-1) and tumour necrosis factor (TNF) levels in proliferative diabetic retinopathy. *Eye* 2006;20:1366–1369
- Joussen AM, Poulaki V, Mitsiades N, Kirchhof B, Koizumi K, Döhmen S, Adamis AP. Nonsteroidal anti-inflammatory drugs prevent early diabetic retinopathy via TNF-alpha suppression. *FASEB J* 2002;16:438–440
- Bamforth SD, Lightman SL, Greenwood J. Ultrastructural analysis of interleukin-1 beta-induced leukocyte recruitment to the rat retina. *Invest Ophthalmol Vis Sci* 1997;38:25–35
- Kowluru RA, Odenbach S. Role of interleukin-1beta in the development of retinopathy in rats: effect of antioxidants. *Invest Ophthalmol Vis Sci* 2004;45:4161–4166
- Ben-Mahmud BM, Mann GE, Datti A, Orlacchio A, Kohner EM, Chibber R. Tumour necrosis factor-alpha in diabetic plasma increases the activity of core 2 GlcNAc-T and adherence of human leukocytes to retinal endothelial cells: significance of core 2 GlcNAc-T in diabetic retinopathy. *Diabetes* 2004;53:2968–2976
- Saishin Y, Saishin Y, Takahashi K, Melia M, Vinore SA, Campochiaro PA. Inhibition of protein kinase C decreases prostaglandin-induced breakdown of the blood-retinal barrier. *J Cell Physiol* 2003;195:210–219
- Matter K, Balda MS. Signalling to and from tight junctions. *Nat Rev Mol Cell Biol* 2003;4:225–236
- Antonetti DA, Barber AJ, Khin S, Lieth E, Tarbell JM, Gardner TW. Vascular permeability in experimental diabetes is associated with reduced endothelial occludin content: vascular endothelial growth factor decreases occludin in retinal endothelial cells. *Penn State Retina Research Group. Diabetes* 1998;47:1953–1959
- Barber AJ, Antonetti DA. Mapping the blood vessels with paracellular permeability in the retinas of diabetic rats. *Invest Ophthalmol Vis Sci* 2003;44:5410–5416
- Gardner TW. Histamine, ZO-1 and increased blood-retinal barrier permeability in diabetic retinopathy. *Trans Am Ophthalmol Soc* 1995;93:583–621
- Tomi M, Hosoya K. Application of magnetically isolated rat retinal vascular endothelial cells for the determination of transporter gene expression levels at the inner blood-retinal barrier. *J Neurochem* 2004;91:1244–1248
- Antonetti DA, Barber AJ, Hollinger LA, Wolpert EB, Gardner TW. Vascular endothelial growth factor induces rapid phosphorylation of tight junction proteins occludin and zonula occluden 1. A potential mechanism for vascular permeability in diabetic retinopathy and tumors. *J Biol Chem* 1999;274:23463–23467
- Harhaj NS, Felinski EA, Wolpert EB, Sundstrom JM, Gardner TW, Antonetti DA. VEGF activation of protein kinase C stimulates occludin phosphorylation and contributes to endothelial permeability. *Invest Ophthalmol Vis Sci* 2006;47:5106–5115
- Murakami T, Felinski EA, Antonetti DA. Occludin phosphorylation and ubiquitination regulate tight junction trafficking and vascular endothelial growth factor-induced permeability. *J Biol Chem* 2009;284:21036–21046
- Nitta T, Hata M, Gotoh S, Seo Y, Sasaki H, Hashimoto N, Furuse M, Tsukita S. Size-selective loosening of the blood-brain barrier in claudin-5-deficient mice. *J Cell Biol* 2003;161:653–660
- Umeda K, Ikenouchi J, Katahira-Tayama S, Furuse K, Sasaki H, Nakayama M, Matsui T, Tsukita S, Furuse M, Tsukita S. ZO-1 and ZO-2 independently determine where claudins are polymerized in tight-junction strand formation. *Cell* 2006;126:741–754
- Katsuno T, Umeda K, Matsui T, Hata M, Tamura A, Itoh M, Takeuchi K, Fujimori T, Nabeshima Y, Noda T, Tsukita S, Tsukita S. Deficiency of zonula occludens-1 causes embryonic lethal phenotype associated with defected yolk sac angiogenesis and apoptosis of embryonic cells. *Mol Biol Cell* 2008;19:2465–2475
- Antonetti DA, Wolpert EB. Isolation and characterization of retinal endothelial cells. *Methods Mol Med* 2003;89:365–374
- Xu Q, Qaum T, Adamis AP. Sensitive blood-retinal barrier breakdown quantitation using Evans blue. *Invest Ophthalmol Vis Sci* 2001;42:789–794
- VanGuilder HD, Brucklacher RM, Patel K, Ellis RW, Freeman WM, Barber AJ. Diabetes downregulates presynaptic proteins and reduces basal synapsin I phosphorylation in rat retina. *Eur J Neurosci* 2008;28:1–11
- Livak KJ, Schmittgen TD. Analysis of relative gene expression data using real-time quantitative PCR and the 2(-Delta Delta C(T)) Method. *Methods* 2001;25:402–408
- Harhaj NS, Barber AJ, Antonetti DA. Platelet-derived growth factor mediates tight junction redistribution and increases permeability in MDCK cells. *J Cell Physiol* 2002;193:349–364
- Barber AJ, Antonetti DA, Gardner TW. Altered expression of retinal occludin and glial fibrillary acidic protein in experimental diabetes. The

- Penn State Retina Research Group. *Invest Ophthalmol Vis Sci* 2000;41:3561–3568
34. Bobrovnikova-Marjon EV, Marjon PL, Barbash O, Vander Jagt DL, Abcouwer SF. Expression of angiogenic factors vascular endothelial growth factor and interleukin-8/CXCL8 is highly responsive to ambient glutamine availability: role of nuclear factor-kappaB and activating protein-1. *Cancer Res* 2004;64:4858–4869
  35. Mahajan DK, London SN. Mifepristone (RU486): a review. *Fertil Steril* 1997;68:967–976
  36. Felinski EA, Cox AE, Phillips BE, Antonetti DA. Glucocorticoids induce transactivation of tight junction genes occludin and claudin-5 in retinal endothelial cells via a novel cis-element. *Exp Eye Res* 2008;86:867–878
  37. Leitges M, Sanz L, Martin P, Duran A, Braun U, García JF, Camacho F, Diaz-Meco MT, Rennert PD, Moscat J. Targeted disruption of the zetaPKC gene results in the impairment of the NF-kappaB pathway. *Mol Cell* 2001;8:771–780
  38. Chou MM, Hou W, Johnson J, Graham LK, Lee MH, Chen CS, Newton AC, Schaffhausen BS, Toker A. Regulation of protein kinase C zeta by PI 3-kinase and PDK-1. *Curr Biol* 1998;8:1069–1077
  39. Zhang R, Xu Y, Ekman N, Wu Z, Wu J, Alitalo K, Min W. Etk/Bmx transactivates vascular endothelial growth factor 2 and recruits phosphatidylinositol 3-kinase to mediate the tumor necrosis factor-induced angiogenic pathway. *J Biol Chem* 2003;278:51267–51276
  40. Carmo A, Cunha-Vaz JG, Carvalho AP, Lopes MC. Effect of cyclosporin-A on the blood-retinal barrier permeability in streptozotocin-induced diabetes. *Mediators Inflamm* 2000;9:243–248
  41. Leal EC, Manivannan A, Hosoya K, Terasaki T, Cunha-Vaz J, Ambrósio AF, Forrester JV. Inducible nitric oxide synthase isoform is a key mediator of leukostasis and blood-retinal barrier breakdown in diabetic retinopathy. *Invest Ophthalmol Vis Sci* 2007;48:5257–5265
  42. Förster C, Burek M, Romero IA, Weksler B, Couraud PO, Drenckhahn D. Differential effects of hydrocortisone and TNFalpha on tight junction proteins in an in vitro model of the human blood-brain barrier. *J Physiol* 2008;586:1937–1949
  43. Burek M, Förster CY. Cloning and characterization of the murine claudin-5 promoter. *Mol Cell Endocrinol* 2009;298:19–24
  44. Mankertz J, Tavalali S, Schmitz H, Mankertz A, Riecken EO, Fromm M, Schulzke JD. Expression from the human occludin promoter is affected by tumor necrosis factor alpha and interferon gamma. *J Cell Sci* 2000;113:2085–2090
  45. Sundstrom JM, Tash BR, Murakami T, Flanagan JM, Bewley MC, Stanley BA, Gonsar KB, Antonetti DA. Identification and analysis of occludin phosphosites: a combined mass spectrometry and bioinformatics approach. *J Proteome Res* 2009;8:808–817
  46. Criswell TL, Arteaga CL. Modulation of NFkappaB activity and E-cadherin by the type III transforming growth factor beta receptor regulates cell growth and motility. *J Biol Chem* 2007;282:32491–32500
  47. Julien S, Puig I, Caretti E, Bonaventure J, Nelles L, van Roy F, Dargemont C, de Herreros AG, Bellacosa A, Larue L. Activation of NF-kappaB by Akt upregulates Snail expression and induces epithelium mesenchyme transition. *Oncogene* 2007;26:7445–7456
  48. Batlle E, Sancho E, Francí C, Domínguez D, Monfar M, Baulida J, García De Herreros A. The transcription factor snail is a repressor of E-cadherin gene expression in epithelial tumour cells. *Nat Cell Biol* 2000;2:84–89
  49. Ikenouchi J, Matsuda M, Furuse M, Tsukita S. Regulation of tight junctions during the epithelium-mesenchyme transition: direct repression of the gene expression of claudins/occludin by Snail. *J Cell Sci* 2003;116:1959–1967
  50. Martínez-Estrada OM, Cullerés A, Soriano FX, Peinado H, Bolós V, Martínez FO, Reina M, Cano A, Fabre M, Vilaró S. The transcription factors Slug and Snail act as repressors of Claudin-1 expression in epithelial cells. *Biochem J* 2006;394:449–457
  51. Anrather J, Csizmadia V, Soares MP, Winkler H. Regulation of NF-kappaB RelA phosphorylation and transcriptional activity by p21(ras) and protein kinase Czeta in primary endothelial cells. *J Biol Chem* 1999;274:13594–13603
  52. Frey RS, Gao X, Javaid K, Siddiqui SS, Rahman A, Malik AB. Phosphatidylinositol 3-kinase gamma signaling through protein kinase Czeta induces NADPH oxidase-mediated oxidant generation and NF-kappaB activation in endothelial cells. *J Biol Chem* 2006;281:16128–16138
  53. Garin G, Abe J, Mohan A, Lu W, Yan C, Newby AC, Rhaman A, Berk BC. Flow antagonizes TNF-alpha signaling in endothelial cells by inhibiting caspase-dependent PKC zeta processing. *Circ Res* 2007;101:97–105
  54. Aiello LP, Bursell SE, Clermont A, Duh E, Ishii H, Takagi C, Mori F, Ciulla TA, Wasy K, Jirousek M, Smith LE, King GL. Vascular endothelial growth factor-induced retinal permeability is mediated by protein kinase C in vivo and suppressed by an orally effective beta-isoform-selective inhibitor. *Diabetes* 1997;46:1473–1480